

PACS numbers: 42.55.Wd; 42.60.Fc; 42.65.Re
DOI: 10.1070/QE2012v042n05ABEH014797

High-power thulium-doped fibre laser with intracavity dispersion management

A.A. Krylov, M.A. Chernysheva, D.S. Chernykh, A.K. Senatorov, I.M. Tupitsyn, P.G. Kryukov, E.M. Dianov

Abstract. **This paper reports a scheme for the generation and amplification of pico- and femtosecond pulses in the range 1.93–1.97 μm using thulium-doped silica fibres. Group velocity dispersion (GVD) management in the cavity of the thulium-doped fibre laser oscillator is ensured by a single-mode germanosilicate fibre (75 mol% GeO_2 in the core) with a positive GVD. Pulses are obtained down to 200 fs in duration and up to 56 nJ in energy.**

Keywords: *thulium-doped optical fibre, mode locking, GVD compensation, fibre amplifier, soliton.*

1. Introduction

There is currently increasing interest in fibre lasers generating ultrashort (femto- and picosecond) pulses (USPs) in various spectral regions. Particular attention is paid to thulium-doped active fibres, which are capable of lasing at wavelengths around 2 μm. The reason for the increased interest in USP lasers is that they have considerable potential for use in medicine, spectroscopy, laser radar systems and micromachining of transparent materials, including semiconductors [1–4].

In the 2-μm range, silica fibres typically have an anomalous group velocity dispersion (GVD), so thulium-doped fibre lasers without intracavity GVD management operate in the soliton regime [5–7]. Intracavity GVD management enables control over lasing regimes and the generation of pulses with a spectral shape, duration and energy variable in rather wide ranges [8, 9]. One such regime is dispersion-managed (DM) soliton generation [9]. In contrast to the energy of the fundamental soliton, which is strictly limited because the anomalous GVD is compensated for by self-phase modulation in the fibre [10], the DM soliton energy can be considerably increased. Moreover, DM solitons are generated even at zero net intracavity GVD, where solitons are unstable [10].

Wang et al. [11] were the first to demonstrate an all-fibre thulium laser in which the amount and sign of intracavity GVD were controlled through the incorporation of a 2-m length of fibre with a normal (positive) GVD $\beta_2 = +900$ ps^2 km^{-1} into the cavity. This allowed them to obtain 235-fs 4.8-nJ pulses. At the same time, Wang et al. [11] reported nothing about the possible range of laser pulse energies or durations corresponding to changes in the length of the GVD-compensating fibre.

This paper presents a passively mode-locked thulium-doped fibre laser with intracavity GVD management ensured by a low-loss single-mode germanosilicate fibre with a normal GVD in the 2-μm range. We demonstrate that the laser pulse duration and the shape of the laser emission spectrum can be effectively controlled by varying the amount and sign of intracavity GVD. In addition, we demonstrate pulse amplification in a multimode-diode-pumped thulium–ytterbium codoped fibre, accompanied by pulse compression.

2. Thulium-fibre pulse generator

Figure 1 shows the configuration of a thulium-doped fibre laser oscillator. A 1560-nm pump beam from an erbium–ytterbium fibre laser was coupled into the cavity of the thulium-doped fibre laser using a fibre multiplexer. The gain medium of the laser was a 68-cm length of isotropic step-index fibre doped with thulium and aluminium ($\Delta n = 0.012$, core diameter $d \approx 10$ μm, 0.8 wt% thulium, 3.6 wt% aluminium, cutoff wavelength $\lambda_c \approx 2.2$ μm). The unsaturated absorption in the fibre at the pump wavelength was 60 dB m^{-1}.

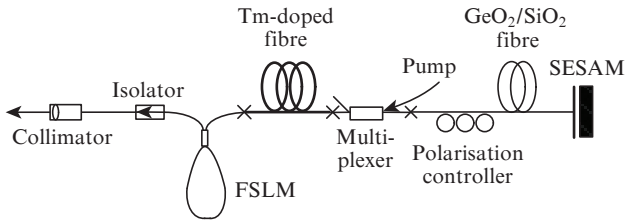

Figure 1. Passively mode-locked thulium-doped fibre laser with intracavity GVD management.

Measurements of the dispersion parameter $D = -(2\pi c/\lambda^2)\beta_2$, where c is the speed of light in vacuum, showed that D varied monotonically in the spectral range 1200–2100 nm ($\beta_2 = -81$ ps^2 km^{-1} at $\lambda = 1960$ nm).

The cavity of the thulium-doped fibre laser was formed by a 1960-nm 58% reflecting fibre Sagnac loop mirror (FSLM) and a semiconductor saturable absorber mirror (SESAM) [6, 12]. The latter ensured stable cw passively mode-locked laser operation.

The anomalous GVD introduced by the thulium-doped active fibre and the SMF-28 passive fibre ($\beta_2 = -75$ ps^2 km^{-1} at $\lambda = 1960$ nm) used to fabricate the multiplexer and FSLM was compensated using a single-mode low-loss (under 20 dB km^{-1}

A.A. Krylov, M.A. Chernysheva, D.S. Chernykh, A.K. Senatorov, I.M. Tupitsyn, P.G. Kryukov, E.M. Dianov Fiber Optics Research Center, Russian Academy of Sciences, ul. Vavilova 38, 119333 Moscow, Russia; e-mail: kryukov@fo.gpi.ru

Received 14 December 2011; revision received 16 February 2012
Kvantovaya Elektronika **42** (5) 427–431 (2012)
Translated by O.M. Tsarev

at $\lambda = 1960$ nm) germanosilicate (GeO_2/SiO_2) fibre with a normal GVD ($\beta_2 = +280$ ps^2 km^{-1} at $\lambda = 1960$ nm) [13]. The GeO_2/SiO_2 fibre had a core less than 2 μm in diameter, containing 75 mol% GeO_2 ($\Delta n \approx 0.11$, fundamental-mode diameter $d_{\text{eff}} \approx 3.4$ μm at 1960 nm [14]). The measured second order mode cutoff wavelength of that fibre was ~970 nm. One of the end faces of the germanosilicate fibre was perpendicularly polished and butted directly against the surface of the SESAM, which considerably facilitated its alignment.

The light polarisation in the cavity was varied using a fibre polarisation controller (PC) which employed birefringence induced by independent local compression of the germanosilicate fibre along two axes 45° apart. The PC increased the cavity loss because of the very strong compression of the GeO_2/SiO_2 fibre, which in turn might influence the pulse duration and energy and the shape of the laser emission spectrum. Owing to accurate PC adjustment, stable cw passively mode-locked laser operation was achieved at various GeO_2/SiO_2 fibre lengths and pump powers.

The laser output was passed through an integrated fibre isolator, collimated by a silicon lens system to a diameter of ~1 mm and directed to the measuring system.

3. Results and discussion

Stable single-pulse cw passive mode locking (Fig. 2) was achieved at germanosilicate fibre lengths $L_{\text{Ge}} \leqslant 1$ m.

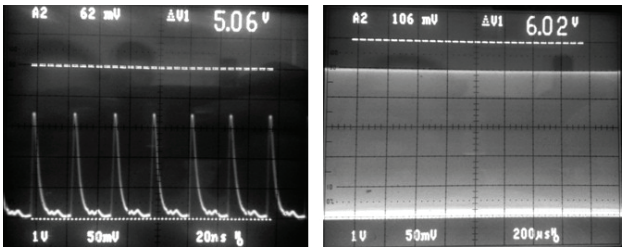

a b

Figure 2. Oscilloscope traces of a train of stable pulses generated by the thulium-doped fibre laser.

Figure 3a shows the intensity autocorrelation traces (ACTs) of laser pulses at different L_{Ge} values and a pump power $P_{\text{pump}} = 250$ mW. The corresponding emission spectra are displayed in Fig. 3b. The net intracavity GVD, D_2, varied from +0.15 to –0.11 ps^2, with zero crossing, and the pulse repetition rate increased from 36.8 to 60.2 MHz.

At fibre lengths $L_{\text{Ge}} = 1$ and 0.42 m, corresponding to $D_2 = +0.15$ and –0.02 ps^2, we observed the generation of picosecond pulses with a narrow, smooth, featureless spectrum [Fig. 3, spectra (*1*), (*2*)]. Least squares fitting of the measured pulse intensity ACTs and the corresponding emission spectra showed that the data were well represented by Gaussians (deviation less than 2%).

In both cases, the laser pulse duration, $\Delta\tau_p$, was 4.8 ps, and the corresponding spectral width (full width at half maximum) was 1.45 and 1.44 nm. Therefore, the time–bandwidth product (the product of the spectral width $\Delta\nu$ and duration of a pulse) was $C = \Delta\nu\,\Delta\tau_p \approx 0.55$ ($C = 0.44$ for transform-limited Gaussian pulses [15]). It is worth noting that the ability to tune the centre wavelength by varying L_{Ge} is due to the associated variation in the polarisation of the light in the cavity.

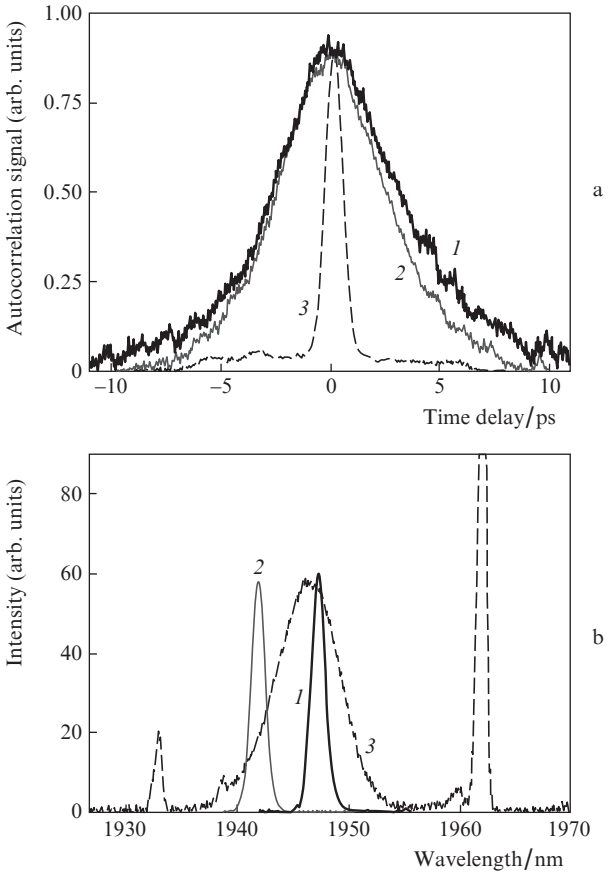

Figure 3. (a) Pulse intensity ACTs and (b) corresponding emission spectra of the thulium-doped fibre laser at different germanosilicate fibre lengths (L_{Ge}) in the cavity: (*1*) $L_{\text{Ge}} = 1$ m, $D_2 \approx +0.15$ ps^2, $\Delta\tau_p \approx 4.8$ ps, bandwidth $\Delta\lambda = 1.45$ nm FWHM, average output power $P_{\text{out}} = 10$ mW; (*2*) $L_{\text{Ge}} = 0.42$ m, $D_2 \approx -0.02$ ps^2, $\Delta\tau_p \approx 4.8$ ps, $\Delta\lambda = 1.44$ nm, $P_{\text{out}} = 11$ mW; (*3*) $L_{\text{Ge}} = 0.07$ m, $D_2 \approx -0.11$ ps^2, $\Delta\tau_p \approx 720$ fs, $\Delta\lambda = 6.3$ nm, $P_{\text{out}} = 11.4$ mW.

Reducing the pump power had no significant effect on the pulse duration, whereas the spectral width of the pulses decreased slightly, which made the pulses almost transform-limited.

Thus, in the case of normal and near-zero GVD, we observed the generation of broad, almost transform-limited Gaussian pulses, whose duration was essentially energy-independent.

The transition to the region of anomalous intracavity GVD ($D_2 \approx -0.11$ ps^2), which took place when the germanosilicate fibre length was reduced to 0.07 m, led to laser operation in the soliton regime. Its characteristic feature is that the laser emission spectrum contains sharp Kelly sidebands [Fig. 3b, spectrum (*3*)] [16] about 15 nm from the centre wavelength. It is worth noting that the net intracavity GVD evaluated from the position of the second-order Kelly sidebands [16] is $D_2 = -0.14$ ps^2, in reasonable agreement with the above value of D_2 (–0.11 ps^2).

Fitting the pulse intensity autocorrelation data with a curve corresponding to a soliton gives an FWHM of 1.12 ps. This corresponds to a soliton width $\Delta\tau_p \approx 720$ fs. At a spectral width $\Delta\lambda = 6.3$ nm, the time–bandwidth product of the pulses is $C \approx 0.36$ ($C = 0.315$ for the fundamental soliton). This means that the pulses are similar in characteristics to fundamental solitons.

The pump power influences the pulse duration according to the relation characteristic of solitons: $\Delta\tau_p \cup 1/E_p$ [8].

An important feature of the ACT represented by curve (*3*) in Fig. 3a is the extended pedestal about 15 ps in width, which accounts, according to our estimates, for about 25% of the pulse energy. We attribute the pedestal to the long relaxation time of the low-loss state of the SESAM, well in excess of the pulse duration, which leads to the formation of an insufficiently sharp trailing edge of the pulse and even produces weaker satellite pulses [12, 17].

In the vicinity of the zero-GVD point, both pico- and femtosecond pulses can be generated, depending on PC settings, as illustrated in Figs 3 and 4. The germanosilicate fibre length was 0.42 and 0.26 m, which corresponded to a net intracavity GVD of –0.02 and –0.06 ps^2. In the former case, the duration of Gaussian pulses was 4.8 and 5.9 ps, with a spectral width of 1.44 and 1.39 nm, respectively. In the latter case, the emission bandwidth increased to 11.5 nm [Fig. 4b, spectrum (*2*)], whereas the duration of Gaussian pulses decreased to 720 fs. The pulse intensity ACT [Fig. 4a, curve (*2*)] also had an extended pedestal, like in the case of soliton generation.

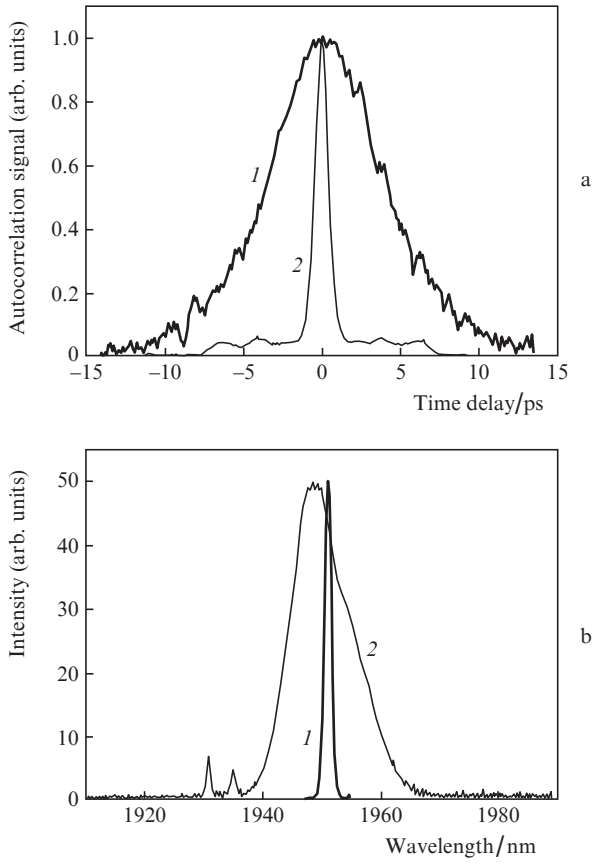

Figure 4. (a) Pulse intensity ACTs and (b) corresponding emission spectra of the thulium-doped fibre laser at $L_{Ge} = 0.26$ m and different PC settings: (*1*) $D_2 \approx -0.06$ ps^2, $\Delta\tau_p \approx 5.9$ ps, $\Delta\lambda = 1.39$ nm, $C = 0.65$, $P_{out} = 11.1$ mW; (*2*) $D_2 \approx -0.06$ ps^2, $\Delta\tau_p \approx 720$ fs, $\Delta\lambda = 11.5$ nm, $C = 0.66$, $P_{out} = 12.3$ mW.

However, in the case of femtosecond pulse generation the sharp sidebands, spaced symmetrically about the central peak and characteristic of solitons, are missing in the emission spectrum. Moreover, reducing the average power (and hence the laser pulse energy) by a factor of 2 (to $P_{out} = 5.2$ mW) decreased the pulse duration to about 710 fs and increased the emission bandwidth to ~14 nm, with no significant changes in shape, which significantly distinguishes such pulses from fundamental solitons. Thus, the pulse under consideration can be thought of as an example of a DM soliton.

A laser with an inertial saturable absorber tends to generate pulses with a duration that corresponds to the relaxation time of its bleached state. However, the pulse duration can be reduced by optimising the relationship between the gain and loss in the cavity [17, 18]. In our case, the polarisation controller compressing the germanosilicate fibre might cause an extra loss, which in turn might ensure optimal conditions for pulse compression. It is worth noting that this effect was observed as well at other germanosilicate fibre lengths, but only in the normal or near-zero anomalous GVD region.

Thus, we have built and investigated an all-fibre thulium laser whose parameters can be varied through intracavity GVD management. The laser pulse duration varies in the range 0.71–6 ps in going from the anomalous to the normal net intracavity GVD region.

4. USP amplification

Figure 5 shows a schematic of a laser pulse amplifier. The thulium fibre laser output was passed through a fibre-optic isolator to an active silica-based fibre with a multicomponent first cladding (MFC) [19] and a core doped with thulium (0.8 wt%), ytterbium (4.8 wt%) and aluminium (2.3 wt%) (core diameter d = 10 μm, Δn = 0.017, cutoff wavelength λ_{cut} = 2.7 μm, fundamental-mode diameter $d_{eff} \approx 9$ μm at λ = 1960 nm).

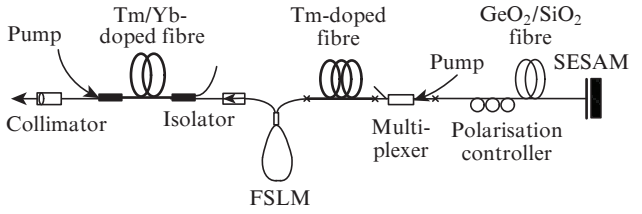

Figure 5. Single-stage fibre amplifier of ultrashort thulium laser pulses.

The fibre had an anomalous GVD which was estimated at about –85 ps^2 km^{-1} (similar to the GVD introduced by the thulium-doped fibre of the master oscillator), with a nonlinearity coefficient of the fibre $\gamma = 1.1$ W^{-1} km^{-1}.

In this study, we used a 5-m length of MFC fibre, which was pumped by multimode light on the ytterbium $^2F_{5/2} \rightarrow {}^2F_{7/2}$ transition at λ = 970–975 nm (up to 17 W of pump power). The excitation energy was then transferred to a thulium ion, which decayed nonradiatively to a metastable sublevel of the $^3H_4$ multiplet [20].

To increase the pump absorption coefficient and, hence, the amplifier efficiency (the slope efficiency of the amplifier was 12%), the pump wavelength should correspond to the absorption peak of the Yb^{3+} ion in silica fibres ($\lambda \approx 975$ nm). This was ensured by adjusting the temperature of the pump diode module using a Peltier element, capable of heating and cooling the module (the laser diode wavelength increases with temperature).

Through an SMF-28 fibre pigtailed (about 0.5 m) collimator, which ensured a back-reflection level of –60 dB, the

amplified light was outcoupled and directed to the measuring system described above.

Figure 6 shows intensity ACTs of amplified pulses and the corresponding emission spectra at different germanosilicate fibre lengths in the cavity of the master oscillator.

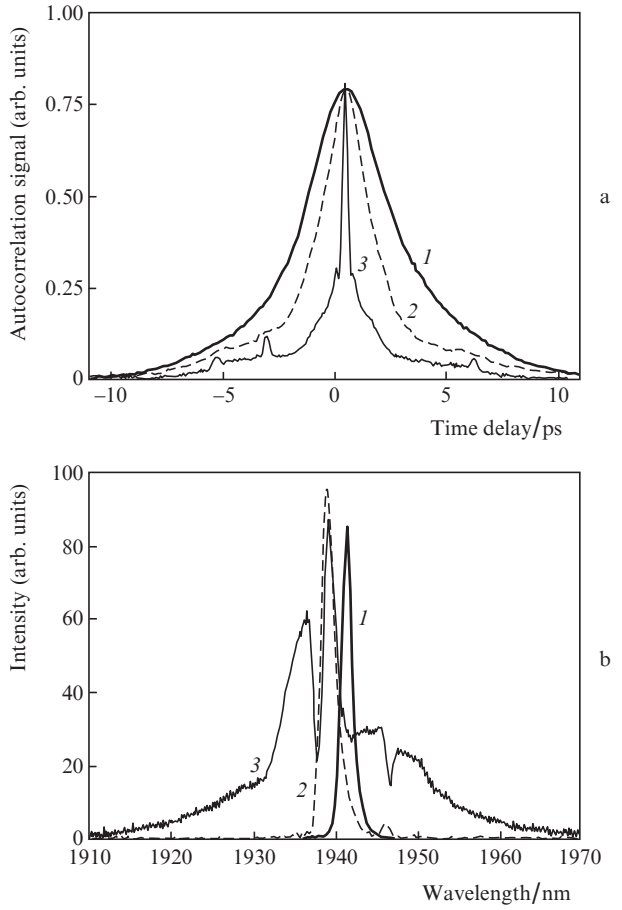

Figure 6. (a) Intensity ACTs of amplified pulses and (b) corresponding emission spectra: (*1*) $L_{Ge} = 1$ m, $D_2 \approx +0.15$ ps^2, $\Delta\tau_a \approx 4.8$ ps, $\Delta\tau_p \approx 3.4$ ps (fitting with a Gaussian), $\Delta\lambda = 2.2$ nm, $C \approx 0.6$, average output power $P_{out} = 1.1$ W; (*2*) $L_{Ge} = 0.6$ m, $D_2 \approx +0.03$ ps^2, $\Delta\tau_a \approx 3$ ps, $\Delta\tau_p \approx 1.9$ ps, $\Delta\lambda = 2.2$ nm, $C = 0.35$ (fitting with a soliton function), $P_{out} = 90$ mW; (*3*) $L_{Ge} = 0.6$ m, $\Delta\tau_a \approx 308$ fs, $\Delta\tau_p \approx 200$ fs (fitting with a soliton function), $P_{out} = 0.62$ W.

At GeO_2/SiO_2 fibre lengths $L_{Ge} = 0.5-1$ m, amplification was observed to reduce the pulse duration from picoseconds to a fraction of a picosecond. At smaller L_{Ge}, around the zero intracavity GVD point, the pulse duration increased again to picoseconds. Thus, the increase in pulse energy in the amplifier was accompanied by pulse compression.

At $L_{Ge} = 1$ m, the width of the pulse intensity ACT, $\Delta\tau_a$, was 4.8 ps [Fig. 6a, curve (*1*)], which corresponded to a 3.4-ps duration of Gaussian pulses, with a spectral width $\Delta\lambda = 2.2$ nm [Fig. 6b, spectrum (*1*)]. At a pump power of 9 W, the average output power of the amplifier was 1.1 W, which corresponded to a 31-nJ energy of the amplified pulses and a peak pulse power of about 9 kW.

When propagating through the amplifier, an input pulse ($\Delta\tau_p \approx 4.5$ ps, $\Delta\lambda \approx 1.5$ nm) with a slight positive frequency modulation acquires an additional positive chirp which is caused by self-phase modulation (SPM) and cannot be fully compensated by the anomalous GVD of the Tm/Yb-doped active fibre and SMF-28 passive fibre at the amplifier output [21]. As a result, the time–bandwidth product of the pulses increases ($C \approx 0.6$ instead of the initial 0.5). In addition, SPM leads to a slight broadening of the emission spectrum, which in turn contributes to pulse compression due to the anomalous GVD in the amplifier. Indeed, when propagating in the anomalous GVD regime, an amplified pulse behaves as a higher order soliton, which compresses in the initial stage of propagation, with concurrent broadening of the spectrum [21].

At a GeO_2/SiO_2 fibre length of 0.6 m, the pulse intensity ACT and emission spectrum had a rather complex shape [Figs 6a, 6b, curves (*3*)] [21, 22]. The pulse intensity ACT comprises a central, compressed peak of 308-fs width, an uncompressed portion about 2 ps in width and a pedestal ~20 ps in width, which we believe to be related to both the quality of the output pulses of the master oscillator and the distinctive features of higher order soliton propagation in fibres [21, 22].

Fitting the central peak of the pulse intensity ACT with a curve representing a soliton gives a soliton width $\Delta\tau_p \approx 200$ fs, which corresponds to pulse compression by about a factor of 10. According to our estimates, the central peak accounts for about 20% of the pulse energy. The uncompressed part of the pulse, which is slightly modulated near the emission peak, accounts for most of the pulse energy. The average power of

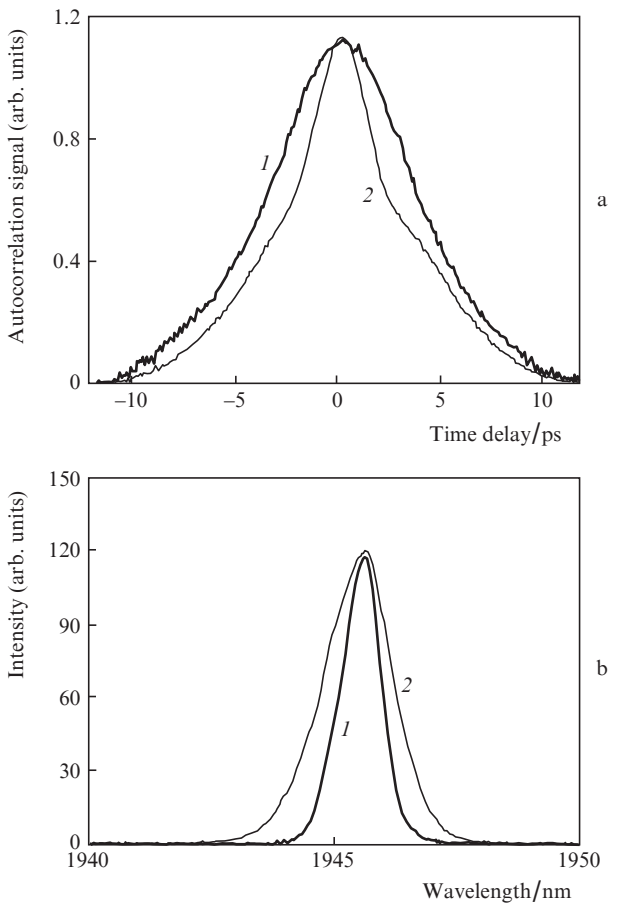

Figure 7. (a) Intensity ACTs of amplified pulses and (b) corresponding emission spectra at $L_{Ge} = 1$ m and different pump powers: (*1*) $P_{pump} = 3.2$ W, $\Delta\tau_a \approx 9$ ps, $\Delta\tau_p \approx 6.4$ ps, $\Delta\lambda = 1$ nm, $C \approx 0.5$, $P_{out} = 0.2$ W; (*2*) $P_{pump} = 17$ W, $\Delta\tau_a \approx 5.7$ ps, $\Delta\tau_p \approx 4$ ps, $\Delta\lambda = 1.7$ nm, $C \approx 0.54$, $P_{out} = 2$ W.

the amplified light is here 0.62 W, which corresponds to a pulse energy of ~15 nJ.

Increasing the pump power to 17 W at L_{Ge} = 1 m, we achieved the highest average power of the amplified light, ~2 W, at a pulse intensity ACT width $\Delta\tau_a \approx 5.7$ ps [Fig. 7a, curve (*2*)]. This corresponded to the highest pulse energy: 56 nJ. Even though the shape of the pulse intensity autocorrelation trace differed somewhat from a Gaussian one, the emission spectrum [Fig. 7b, curve (*2*)], having a FWHM $\Delta\lambda = 1.7$ nm, was smooth and featureless, with an almost Gaussian shape.

5. Conclusions

We have demonstrated a pulsed fibre laser and amplifier configuration in the 2-μm range using thulium-doped silica fibres. Intracavity GVD management in the thulium-doped fibre laser was ensured by a single-mode germanosilicate fibre with a positive GVD and low loss in the 2-μm range.

The generation of both pico- and femtosecond pulses was achieved through cw passively mode-locked operation in going from the normal to the anomalous net intracavity GVD region.

The laser pulses were amplified in an active MFC fibre under multimode diode pumping. The core of the fibre was doped with thulium, ytterbium and aluminium ions. We achieved pulse amplification with little distortion of the shape of the pulse intensity autocorrelation function and emission spectrum (the highest pulse energy reached is 56 nJ). Moreover, our results demonstrate the possibility of pulse compression to a duration under 300 fs, in parallel with pulse amplification.

Acknowledgements. We thank O.G. Okhotnikov for fabricating the SESAM and I.A. Bufetov, M.A. Mel'kumov and V.M. Mashinsky for providing the optical fibres. We are deeply grateful to B.L. Davydov for providing the fibre pigtailed collimator and to A.F. Kosolapov and M.S. Astapovich for measuring the group velocity dispersion of the fibres.

This work was supported by the Russian Foundation for Basic Research (Grant No. 09-02-01124-a).

References

1. www.spie.org/x57663.xml.
2. Kadwani P., Sims R.A., Baudelet M., Shah L., Richardson M.C., Chia J., Altal F. *Opt. Soc. Am. / FILAS*, **FWB3** (2011).
3. Gattass R.R., Mazur E. *Nat. Photonics*, **2**, 219 (2008).
4. Scott N.J., Cilip C.M., Fried N.M. *IEEE Sel. Top. Quantum Electron.*, **15**, 435 (2009).
5. Renninger W.H., Chong A., Wise F.W. *Phys. Rev. A*, **77**, 023814 (2008).
6. Nelson L.E., Ippen E.P., Haus H.A. *Appl. Phys. Lett.*, **67**, 19 (1995).
7. Kivisto S., Hakulinen T., Guina M., Okhotnikov O.G. *IEEE Photonics Technol. Lett.*, **19**, 934 (2007).
8. Martínez O.E., Fork R.L. *Opt. Lett.*, **9**, 156 (1984).
9. Turitsyn S.K., Shapiro E.G., Medvedev S.B., Fedoruk M.P., Mezentsev V.K. *Opt. Telecom.*, **4**, 145 (2003).
10. Hasegawa A., Tappert F. *Appl. Phys. Lett.*, **23**, 142 (1973).
11. Wang Q., Chen T., Chen K. *Opt. Soc. Am./CLEO/QELS*, **CFK7** (2010).
12. Guina M., Xiang N., Vainionpaa A., Okhotnikov O.G., Sajavaara T., Keinonon J. *Opt. Lett.*, **26**, 1809 (2001).
13. Fleming J.W. *Appl. Opt.*, **23**, 4486 (1984).
14. Dianov E.M., Mashinsky V.M. *J. Lightwave Technol.*, **23**, 3500 (2005).
15. Diels J.-C., Rudolph W. *Ultrashort laser pulse phenomena* (New York: Academic Press, 1996).
16. Kelly S.M. *Electron. Lett.*, **28**, 806 (1992).
17. Paschotta R., Keller U. *Appl. Phys. B*, **73**, 653 (2001).
18. Kärtner F.X., Keller U. *Opt. Lett.*, **20**, 16 (1995).
19. Bufetov I.A., Bubnov M.M., Mel'kumov M.A., Dudin V.V., Shubin A.V., Semenov S.L., Kravtsov K.S., Gur'yanov A.N., Yashkov M.V., Dianov E.M. *Kvantovaya Elektron.*, **35**, 328 (2005) [*Quantum Electron.*, **35**, 328 (2005)].
20. Jackson S.D. *Opt. Lett.*, **28**, 2192 (2003).
21. Stolen R.H., Mollenauer L.F., Tomlinson W.J. *Opt. Lett.*, **8**, 186 (1983).
22. Mollenauer L.F., Stolen R.H., Gordon J.P., Tomlinson W.J. *Opt. Lett.*, **8**, 289 (1983).